human DNA pols. In addition, instead of using radioisotope, we have developed a new fluorescent technique for analyzing translesion synthesis and quantifying the miscoding specificity and frequency using two-phased PAGE (Fig. 3).[22,23] Relative bypass frequencies past the dI lesion were also determined by steady-state kinetic studies.[24,25]

Results

Primer extension reactions catalyzed by human DNA pols on dI-modified DNA template

Using unmodified and dI-modified 38-mer templates, we conducted primer extension reactions in the presence of four 2′-deoxynucleoside triphosphates (dNTPs) and varying amounts of pol α, pol η, or pol κΔC (Fig. 4). Primer extension occurred rapidly on unmodified templates to form fully extended products. With the dI-modified template, primer extension catalyzed by pol α was slightly retarded one base before the lesion (see arrowhead in Fig. 4). However, when pol η or pol κΔC was used, primer extension resulted in fully extended products. No blockage was detected at the dI adduct site. When the amounts of pols were increased, products representing more than 32-mer bases long were produced on the unmodified and dI-modified templates. Blunt-end addition to the fully extended product (33–34-mers) was observed, as reported earlier for *Escherichia coli* and mammalian DNA pols.[26,27]

Miscoding frequencies and specificities of the dI adduct

Translesion synthesis catalyzed by pol α, pol η, or pol κΔC was conducted in the presence of all four dNTPs. The fully extended products (approximately 28–34-mers) past the unmodified or modified adducts were recovered, digested by EcoRI, and subjected to two-phased PAGE for quantitative analysis of base substitutions and deletions as described in Materials and Methods (Fig. 3). A standard mixture of six Alexa Fluor 546 dye (Alexa546)-labeled oligodeoxynucleotides containing dC, dA, dG, or dT opposite the lesion or one- and two-base deletions can be resolved by this method (Fig. 5). The percentage of 2′-deoxynucleoside monophosphate incorporation was normalized to the amount of the starting primer. When an unmodified dA template was used, expected incorporation of dTMP, the correct base, was observed opposite dA (Fig. 5). As indicated by the arrowhead in Fig. 5b, small amounts of unknown products were detected. When pol α was used with a template containing dI, dCMP (83.3% of the starting primers) was exclusively incorporated opposite the lesion. Similarly, pol η and pol κΔC promoted preferential incorporation of dCMP (55.0% and 74.7%, respectively) opposite the lesion. No deletions were detected. Surprisingly, no incorporation of dTMP, the correct base, was detected opposite the dI adduct with all pols, that is, pol α, pol η, and pol κΔC.

AGAAAGGAGA^{Alexa546}
5′CATGCTGATGAATTCCTTCZCTTCTTTCCTCTCCCTTT (Z = dA or dI)

dNTPs
DNA polymerase

GTACGACTACTTAAGGAAGNGAAGAAAGGAGA^{Alexa546} (N = dC,dA,dG,or dT)
5′CATGCTGATGAATTCCTTCZCTTCTTTCCTCTCCCTTT

EcoRI

GGAAGNGAAGAAAGGAGA^{Alexa546}
AATTCCTTCZCTTCTTTCCTCTCCCTTT

GGAAG [C / A / G / T / Δ^1] GAAGAAAGGAGA^{Alexa546}
GGAA [Δ^2]

Δ^2C Δ^1 TAG
-urea -urea +urea

Fig. 3. Diagram of the fluorescent two-phased PAGE to determine miscoding specificity of DNA adducts. Unmodified and dI-modified 38-mer templates are annealed to either an Alexa546-labeled 10-mer primer or an Alexa546-labeled 12-mer primer. Primer extension reactions catalyzed by DNA pol α, pol η, or pol κΔC were conducted in the presence of four dNTPs. Fully extended products formed during DNA synthesis were recovered from the polyacrylamide gel (30 × 40 × 0.05 cm), annealed with a complementary 38-mer, cleaved with EcoRI, and subjected to a two-phased PAGE (20 × 65 × 0.05 cm), as described in Materials and Methods. To determine miscoding specificity, mobilities of the reaction products were compared with those of 18-mer standards containing dC, dA, dG, or dT opposite the lesion and one-base (Δ^1) or two-base (Δ^2) deletions.

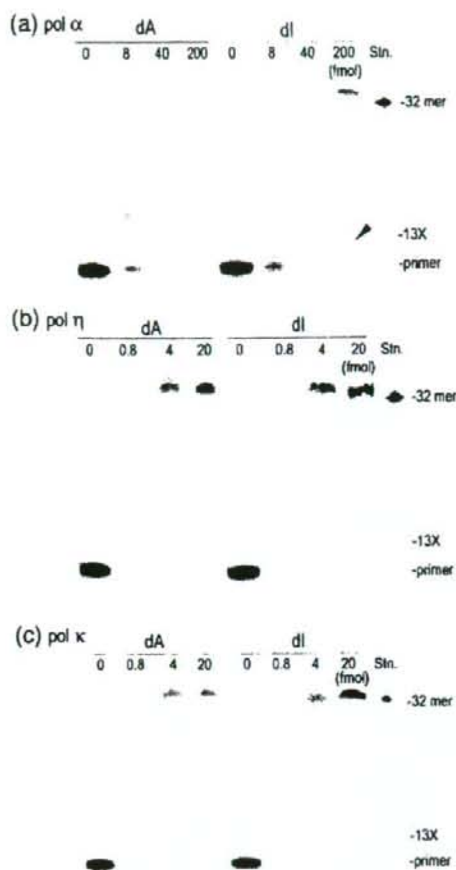

Fig. 4. Primer extension reactions catalyzed by pol α, pol η, or pol κΔC on dI-modified DNA template. Using unmodified or dI-modified 38-mer templates primed with an Alexa546-labeled 10-mer, we performed primer extension reactions at 25 °C for 30 min in a buffer containing four dNTPs (100 μM each) and varying amounts of (a) pol α (0, 8, 40, and 200 fmol), (b) pol η, or (c) pol κΔC (0, 0.8, 4, and 20 fmol), as described in Materials and Methods. The whole amount of the reaction mixture was subjected to 20% denaturing PAGE (30 × 40 × 0.05 cm). An Alexa546-labeled 32-mer (5'AGAGGAAAGTAGCCAAGGAATT-CATCAGCATG) was used as a marker of fully extended product. 13X represents the adducted position

Kinetic studies on dI-modified templates

Steady-state kinetic studies were performed using pol α, pol η, and pol κΔC to determine the frequency of dNTP incorporation (F_{ins}) opposite the dI lesion and chain extension (F_{ext}) from the primer terminus using the same sequence context that was used for the two-phased PAGE assay (Table 1). With pol α, the F_{ins} value for deoxythymidine triphosphate (dTTP) (1.21×10^{-2}), the correct base, opposite the dI was 59 times lower than that for 2'-deoxycytidine triphosphate (dCTP) (0.718). The relative bypass frequency ($F_{ins} \times F_{ext}$) past the dC:dI pair was approximately 2100 times higher than that for the dT:dI pair. F_{ins} and F_{ext} values for dA:dI and dG:dI were not detectable. When pol η was used, the F_{ins} value for dCTP (0.551), the wrong base, opposite the dI was 27 times higher than that for dTTP (2.07×10^{-2}) and was 17 and 75 times higher than that for 2'-deoxyadenosine triphosphate and 2'-deoxyguanosine triphosphate (dGTP), respectively. The F_{ext} value for the dC:dI pair was also higher than that for other 2'-deoxynucleoside monophosphates paired with dI. As a result, the $F_{ins} \times F_{ext}$ value past dC:dI was at least 3 orders of magnitude higher than that past other pairs. Similarly, with pol κ, $F_{ins} \times F_{ext}$ past dC:dI was much higher than that for other base pairs. F_{ins} and F_{ext} values for dTTP were 119 and 55 times lower than that for dCTP, respectively. Thus, all pols, that is, pol α, pol η, and pol κΔC, exclusively promote misincorporation of dCMP opposite the dI lesion during translesion synthesis, since $F_{ins} \times F_{ext}$ values of other dNTPs were considerably lower that that for dCTP, the wrong base.

Discussion

Primer extension reactions catalyzed by DNA pols are a powerful method to explore translesion synthesis past DNA adducts and their accompanying kinetic parameters of nucleotide insertion and extension. A ^{32}P-labeled oligodeoxynucleotide at the 5'-terminus is widely employed in such analyses; however, the handling of hazardous radioisotopes is intricate for use and waste disposal. Indeed, use of radioisotopes is restricted in many countries including Japan. As an alternative to ^{32}P, we used fluorescent dyes, Alexa546 and Cyanin 3 (Cy3), to label the 5'-terminus of the oligodeoxynucleotide used as primers and standard markers. The detection limits of Alexa546- and Cy3-labeled primers were approximately 120 and 240 times lower than that of the ^{32}P-labeled primer, respectively. However, when Alexa546-labeled primers (500 fmol) were annealed with DNA template (750 fmol) and the assays of primer extension and kinetic studies were carried out in this work, the resultant data were quantitative and reproducible (Figs. 6 and 7). Alexa546 exhibits a more sensitive and photostable fluorescence than Cy3. Moreover, even under repeated thawing and melting, an Alexa546-labeled oligomer stored at −20 °C was not degraded for at least 6 months. Using this method, we determined the miscoding frequency and specificity of 8-OxodG, which is known to generate predominantly 2'-deoxyadenosine monophosphate misincorporation at the lesion site. The results obtained from Alexa546 labeling were consistent with that from ^{32}P labeling (data not shown). Thus, Alexa546 was applicable to two-phased PAGE. Therefore, we have used this fluorescent method to explore translesion synthesis past dI adducts and its miscoding specificity and frequency using two-phased PAGE.

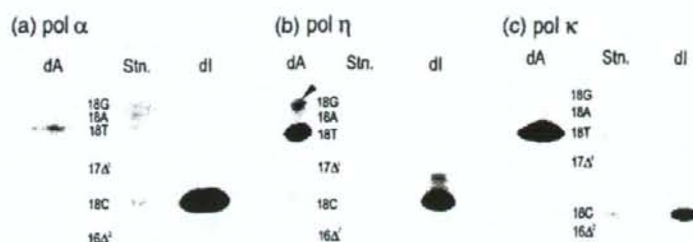

Fig. 5. Miscoding specificities of the dI lesion in reactions catalyzed by pol α, pol η, or pol κΔC. Using unmodified and dI-modified 38-mer templates primed with an Alexa546-labeled 12-mer, we conducted primer extension reactions at 25 °C for 30 min in a buffer containing four dNTPs (100 μM each) and either pol α (200 fmol for unmodified and dI-modified templates), pol κΔC, or pol η (20 fmol for unmodified and dI-modified templates), as described in Materials and Methods. The extended reaction products (>26 bases long) produced on the unmodified and dI-modified templates were extracted following PAGE. The recovered oligodeoxynucleotides were annealed to an unmodified 38-mer and cleaved with EcoRI restriction enzyme, as described in Materials and Methods. The entire product from the unmodified and dI-modified templates was subjected to two-phased PAGE (20 × 65 × 0.05 cm). Mobilities of reaction products were compared with those of 18-mer standards (Fig. 3) containing dC, dA, dG, or dT opposite the lesion and one-base (Δ^1) or two-base (Δ^2) deletions.

The mutation spectrum induced by ˙NO has been investigated in a variety of experimental systems. ˙NO gas showed mutagenicity in TK6 cells[10] and caused predominantly A:T → G:C transitions in plasmids replicated in cultured human and *E. coli* cells[28,29] and C → T transitions in a bacterial system.[9] Moreover, ˙NO-releasing compounds exclusively resulted in G:C → A:T transitions in pSP189 plasmids propagated in human cells.[30] Using similar ˙NO-releasing compounds, $ONOO^-$ caused G:C → T:A and G:C → C:G transversions with the same experimental system.[31,32] Thus, based on the information obtained from these previous reports, the mutation spectrum by ˙NO has not been extensively determined yet.[33] In our previous studies, the miscoding frequencies and specificities of dX, 8-NO_2-dG, and 8-OxodG lesions were quantitatively determined by two-phased PAGE. As a result, 8-NO_2-dG[34] and 8-OxodG[17,35] are miscoding lesions generating primarily G → T transversions (~20% and ~38%, respectively), while the miscoding spectrum of the dX adduct[36] exclusively shows G → A transitions (~50%), which differs from that of 8-NO_2-dG and 8-OxodG. This indicates that each DNA adduct has a unique miscoding specificity and frequency. The mutation spectrum by ˙NO can be hardly determined due to the presence of diverse

Table 1. Kinetic parameters for nucleotide insertion and chain extension reactions catalyzed by human DNA pol α, pol η, and pol κΔC

		Insertion dNTP GAAGAAAGGAGA[Alexa546] 5′CCTTCZCTTCTTTCCTCTCCCTTT			Extension dGTP NGAAGAAAGGAGA[Alexa546] 5′CCTTCZCTTCTTTCCTCTCCCTTT			
	N:Z	K_m (μM)[a]	V_{max} (% min^{-1})[a]	F_{ins}	K_m (μM)[a]	V_{max} (% min^{-1})[a]	F_{ext}	$F_{ins} \times F_{ext}$
Pol α	T:A	0.56±0.03	0.53±0.02	1.0	0.41±0.14	0.31±0.03	1.0	1.0
	C:Z	0.73±0.26	0.47±0.03	0.718	0.48±0.09	0.25±0.01	0.679	0.487
	A:Z	N.D.	N.D.	N.D.	N.D.	N.D.	N.D.	N.D.
	G:Z	N.D.	N.D.	N.D.	N.D.	N.D.	N.D.	N.D.
	T:Z	9.74±1.60	0.11±0.07	1.21×10^{-2}	7.09±1.50	10.1±0.65	1.92×10^{-2}	2.32×10^{-4}
Pol η	T:A	0.65±0.17	5.37±0.26	21.0	0.69±0.13	7.49±0.11	1.0	1.0
	C:Z	1.74±0.58	7.79±0.48	0.351	0.96±0.18	8.44±0.25	0.809	0.446
	A:Z	4.87±1.22	1.28±0.03	3.18×10^{-2}	6.63±0.76	2.66±0.08	3.66×10^{-2}	1.16×10^{-2}
	G:Z	16.1±1.03	1.00±0.01	7.30×10^{-3}	11.6±4.23	1.14±0.11	9.40×10^{-4}	6.86×10^{-5}
	T:Z	7.00±1.97	1.19±0.03	2.07×10^{-2}	6.76±0.41	4.99±0.02	6.72×10^{-2}	1.39×10^{-3}
Pol κΔC	T:A	1.43±0.38	11.1±0.47	1.0	0.55±0.07	13.9±0.54	1.0	1.0
	C:Z	1.36±0.40	10.3±0.44	0.987	0.79±0.76	13.1±0.12	0.651	0.642
	A:Z	15.5±4.30	1.10±0.05	9.23×10^{-3}	10.7±2.43	2.17±0.07	8.13×10^{-4}	7.50×10^{-4}
	G:Z	84.0±15.4	0.76±0.30	1.12×10^{-3}	12.8±2.25	0.51±0.05	1.57×10^{-3}	1.75×10^{-5}
	T:Z	23.5±6.93	1.50±0.11	8.26×10^{-3}	5.28±0.37	1.59±0.03	1.18×10^{-2}	9.74×10^{-5}

Kinetics of nucleotide insertion and chain extension reactions were determined as described in Materials and Methods. Frequencies of nucleotide insertion (F_{ins}) and chain extension (F_{ext}) were estimated by the following equation: $F = (V_{max}/K_m)_{wrong\ pair}/(V_{max}/K_m)_{correct\ pair = dT:dA}$. Z = dA or dI lesion.

N.D., not detectable.

[a] Data are expressed as mean ± SD obtained from three independent experiments.

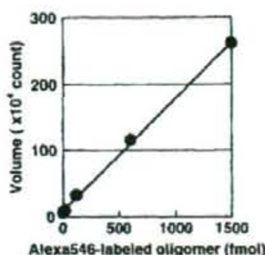

Fig. 6. Calibration curve using fluorescent oligomers labeled by Alexa546. Varying amounts of Alexa546-labeled oligomer were subjected to 20% denaturing PAGE. The volume of bands was quantitatively measured by using Molecular Imager FX Pro and Quantity One software (Bio-Rad) to find a linear range in the fluorescent analysis.

DNA adducts caused by ·NO-involved species (Fig. 1) and its miscoding variety.[17,34,35] Therefore, the quantitative miscoding properties of each ·NO-derived DNA adduct must be required to explore its roles in the inflammation-driven carcinogenesis.

The miscoding specificity of dI was determined by using an *in vitro* experimental system that can quantify base substitutions and deletions formed during replication in the presence of four dNTPs. Pol α, pol η, and pol κΔC incorporated dCMP (83.3%, 55.0%, and 74.7%, respectively) preferentially opposite the dI lesion rather than dTMP, the correct base (Fig. 5). Kamiya *et al.* reported earlier that mouse pol α inserted dCMP and dTMP, the correct base, opposite the dI lesion.[16] In contrast, human pol α promoted direct incorporation of dCMP only (Fig. 5). These indicate that the pols promote miscoding by incorporating dCMP opposite the dI lesion during DNA synthesis. Thus, dI is a highly miscoding lesion, generating A→G transitions in human cells. Steady-state kinetic studies supported these results. When pol α, pol η, and pol κΔC were used, $F_{ins} \times F_{ext}$ values for dC:dI pairs were 2100, 320, and 6600 times higher than those for dT:dI pairs, respectively (Table 1). Therefore, the kinetic results were consistent with that observed using two-phased PAGE analysis. Taken together, both analyses showed that human

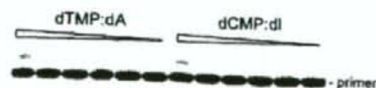

Fig. 7. Typical image of PAGE for kinetic studies performed by Alexa546 labeling. Using unmodified or dI-modified 38-mer templates (750 fmol) primed with an Alexa546-labeled 12-mer (500 fmol), we conducted primer extension reactions at 25 °C for 2 min in a buffer containing pol κΔC (1 fmol) and either dTTP (0.25–25 μM for unmodified templates) or dCTP (0.25–25 μM for dI-modified templates), as described in Materials and Methods. The whole amount of the reaction mixture was subjected to 20% denaturing PAGE (30 × 40 × 0.05 cm).

DNA pols miscode at dI lesions by exclusively incorporating dCMP. The miscoding specificity was consistent with that observed in *E. coli*,[9] mammalian cells,[10,37] and mice exposed to ·NO.[15]

To compare the relative bypass frequency of dI, dX, and 8-NO_2-dG by pol α, pol η, and pol κΔC, these adducts were embedded in a similar sequence context[34,36] (Table 2). With pol α, the $F_{ins} \times F_{ext}$ ratio for the dC:dI/dT:dI pairs was 2100. This number was remarkably higher than that for the dT:dX/dC:dX (ratio = 1.5) or dA:8-NO_2-dG/dC:8-NO_2-dG (ratio = 0.01) pairs. Similar results were observed with pol η and pol κΔC. The ratios of $F_{ins} \times F_{ext}$ past dI were 2 orders of magnitude higher than those of dX and 8-NO_2-dG. Thus, dI adducts promote a higher miscoding potential (A→G transitions) than those of dX or 8-NO_2-dG. However, the highly mutagenic dI lesions did not show serious mutation frequency[9,10] even though they were predominantly paired with the wrong base, dCMP. Endonuclease V (endo V) has shown to be a dI-specific endonuclease.[38–40] Methylpurine glycosylase also recognizes this lesion.[41–43] For instance, *E. coli* cells lacking the endo V (*nfi*) gene were shown to exhibit elevated mutation frequencies when exposed to nitrous acid. The increased mutations were predominantly A:T→G:C mutations, followed by lesser G:C→A:T mutations.[44,45] This indicates that endo V is primarily involved in the repair of dI lesions.[44–48]

The structure of double-stranded oligodeoxynucleotide containing the dI:dC pair was determined by thermodynamic and NMR studies.[49,50] dI can most stably pair with dC among four dNs, and its geometric structure is similar in form with the Watson–Crick structure (Fig. 8). dI has a carbonyl group at position C6 and a positive charge at position N1 after dA suffers from nitrosative deamination by ·NO. Thus, since the structure of dI is similar to that of dG rather than dA, the dI adduct can predominantly pair with dC, the wrong base.

In conclusion, nonradioactive kinetic studies and two-phased PAGE were performed to explore the

Table 2. $F_{ins} \times F_{ext}$ past DNA adducts by human DNA pol α, pol η, and pol κΔC

	Z=	dI[a]	dX[b]	8-NO_2-dG[c]
Pol α	C:Z	**0.487**	4.50×10^{-3}	1.69×10^{-7}
	A:Z	N.D.	2.18×10^{-1}	**1.31×10^{-5}**
	G:Z	N.D.	$1.11 \times 10^{-[illegible]}$	2.63×10^{-6}
	T:Z	2.32×10^{-4}	**6.68×10^{-3}**	5.87×10^{-6}
Pol η	C:Z	**0.446**	3.24×10^{-2}	6.94×10^{-5}
	A:Z	$1.16 \times 10^{-[illegible]}$	1.71×10^{-1}	**5.09×10^{-3}**
	G:Z	6.86×10^{-3}	2.94×10^{-1}	4.63×10^{-4}
	T:Z	1.39×10^{-3}	**0.259**	4.06×10^{-4}
Pol κΔC	C:Z	**0.642**	8.39×10^{-1}	6.37×10^{-5}
	A:Z	7.50×10^{-3}	2.43×10^{-6}	**2.88×10^{-5}**
	G:Z	1.75×10^{-6}	2.48×10^{-6}	2.62×10^{-6}
	T:Z	9.74×10^{-5}	**5.12×10^{-2}**	6.62×10^{-7}

Values in boldface show a primarily misincorporated base opposite the DNA adduct.

N.D., not detectable.

[a] Data were taken from Table 1.

[b] Data were taken from Ref. 36.

[c] Data were taken from Ref. 34.

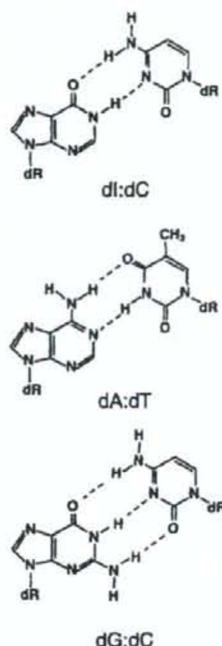

Fig. 8. Possible base pairing of the dI adduct with dC.

miscoding specificities and frequencies of the dI lesion catalyzed by Y-family human DNA pols. The dI adduct represents a highly miscoding lesion capable of generating A→G transitions, indicating that this ˙NO-induced lesion plays an important role in initiating inflammation-driven carcinogenesis.

Materials and Methods

General

Ultrapure dNTPs were from GE Healthcare. EcoRI restriction endonuclease (100 U/μL) was purchased from New England BioLabs. Blue Dextran (D5751) was obtained from Sigma. Human pol α was obtained from CHIMERx (Milwaukee, WI). Human pol η was purified as previously described.[19] Human pol κ (pol κΔC) was overexpressed in *E. coli* and purified as a C-terminally truncated form. The protein has 10× His tag at the N-terminal position and contains 559 amino acids from the N-terminus (N. Niimi and T. Nohmi *et al.*, unpublished results).

Preparation of oligodeoxynucleotides

All oligodeoxynucleotides, Alexa546 (Molecular Probes)-labeled primers, standard markers, and dI-modified template were obtained from Japan Bio Service Co. (Saitama, Japan). Alexa546 was conjugated at the 5'-terminus of primers and standard markers. A single dI was located at the 20th position from the 5'-termini in the modified 38-mer template (5'CATGCTGATGAATTCCTTCZCTTCTTTC-CTCTCCCTTT, where Z is dI). The oligomers were purified by using 20% denaturing PAGE before use.

Primer extension reactions

Primer extension reactions catalyzed by pol α, pol η, or pol κΔC were conducted at 25 °C for 30 min in a buffer (10 μL) containing all four dNTPs (100 μM each) using dI-modified and unmodified 38-mer templates (750 fmol) primed with an Alexa546-labeled 10-mer (500 fmol, 5' AGAGGAAAGA) (Fig. 3). The reaction buffer for pol α contains 40 mM Tris–HCl (pH 8.0), 5 mM $MgCl_2$, 60 mM KCl, 10 mM dithiothreitol, 250 μg/mL bovine serum albumin, and 2.5% glycerol. The reaction buffer for pol η and pol κΔC contains 40 mM Tris–HCl (pH 8.0), 1 mM $MgCl_2$, 10 mM dithiothreitol, 250 μg/mL bovine serum albumin, 60 mM KCl, and 2.5% glycerol. Reaction was stopped by addition of 2 μL formamide dye containing Blue Dextran (100 mg/mL) and ethylenediaminetetraacetic acid (50 mM) and incubation at 95 °C for 3 min. The whole amount of the reaction sample was subjected to 20% denaturing PAGE (30 × 40 × 0.05 cm). The positions of bands and homogeneities of oligodeoxynucleotides following PAGE were determined by using Molecular Imager FX Pro and Quantity One software (Bio-Rad). The linear range to quantitatively detect fluorescence-labeled oligomers was from 5 to 1500 fmol (Fig. 6).

Quantitation of miscoding specificity

Using dI-modified and unmodified 38-mer oligodeoxynucleotide (750 fmol) primed with an Alexa546-labeled 12-mer (500 fmol, 5'AGAGGAAAGAAG), we conducted primer extension reactions catalyzed by pol α (200 fmol), pol η (20 fmol), or pol κΔC (20 fmol) at 25 °C for 30 min in a buffer (10 μL) containing all four dNTPs (100 μM each) and subjected them to 20% denaturing PAGE (30 × 40 × 0.05 cm). Extended reaction products (>26 bases long) were extracted from the gel. The recovered oligodeoxynucleotides were annealed with an unmodified 38-mer, cleaved with EcoRI, and subjected to two-phased PAGE (20 × 65 × 0.05 cm) containing 7 M urea in the upper phase and no urea in the middle and bottom phases (each phase contains 18%, 20%, and 24% polyacrylamide, respectively). The phase width is approximately 10, 37, and 18 cm from the upper phase. To quantify base substitutions and deletions, we compared the mobility of the reaction products with those of Alexa546-labeled 18-mer standards containing dC, dA, dG, or dT opposite the lesion and one-base (Δ^1) or two-base (Δ^2) deletions[17,18] (Fig. 3).

Steady-state kinetic studies of nucleotide insertion and extension

Kinetic parameters associated with nucleotide insertion opposite the dI lesion and chain extension from the 3' primer terminus were determined at 25 °C, using varying amounts of single dNTPs. For insertion kinetics, reaction mixtures containing dNTP (0–250 μM) and either pol α (20–200 fmol), pol η (2–20 fmol), or pol κΔC (1–20 fmol) were incubated at 25 °C for 2 min in 10 μL of Tris–HCl buffer (pH 8.0) using a 38-mer template (750 fmol) primed with an Alexa546-labeled 12-mer (500 fmol; 5'AGAG-

GAAAGAAG). Reaction mixtures containing a 38-mer template (750 fmol) primed with an Alexa546-labeled 13-mer (500 fmol; 5'AGAGGAAAGAAGN, where N is C, A, G, or T), with varying amounts of dGTP (0–250 μM) and either pol α (20–200 fmol), pol η (1–20 fmol), or pol ιΔC (1–20 fmol), were used to measure chain extension. The reaction samples were subjected to 20% denaturing PAGE (30 × 40 × 0.05 cm). The Michaelis constants (K_m) and maximum rates of reaction (V_{max}) were obtained from Hanes–Woolf plots. Frequencies of dNTP insertion (F_{ins}) and chain extension (F_{ext}) were determined relative to the dT:dA base pair according to the following equation: $F = (V_{max}/K_m)_{[wrong\ pair]}/(V_{max}/K_m)_{[correct\ pair = dT:dA]}$.[24,25]

Acknowledgements

This research was supported in part by Grants-in-aid for Scientific Research 19710059 from the Ministry of Education, Culture, Sports, Science and Technology (to M.Y.). This work was also partially supported by Health, Welfare, and Labor Science Research Grants (H18-food-general-009) and a Grant-in-aid (KHB1007) from the Japan Health Science Foundation (to M.H.).

References

1. Ohshima, H. & Bartsch, H. (1994). Chronic infections and inflammatory processes as cancer risk factors: possible role of nitric oxide in carcinogenesis. *Mutat. Res.* **305**, 253–264.
2. Cassell, G. H. (1998). Infectious causes of chronic inflammatory diseases and cancer. *Emerg. Infect. Dis.* **4**, 475–487.
3. Ohshima, H., Tatemichi, M. & Sawa, T. (2003). Chemical basis of inflammation-induced carcinogenesis. *Arch. Biochem. Biophys.* **417**, 3–11.
4. Burney, S., Caulfield, J. L., Niles, J. C., Wishnok, J. S. & Tannenbaum, S. R. (1999). The chemistry of DNA damage from nitric oxide and peroxynitrite. *Mutat. Res.* **424**, 37–49.
5. deRojas-Walker, T., Tamir, S., Ji, H., Wishnok, J. S. & Tannenbaum, S. R. (1995). Nitric oxide induces oxidative damage in addition to deamination in macrophage DNA. *Chem. Res. Toxicol.* **8**, 473–477.
6. Yermilov, V., Rubio, J., Becchi, M., Friesen, M. D., Pignatelli, B. & Ohshima, H. (1995). Formation of 8-nitroguanine by the reaction of guanine with peroxynitrite *in vitro*. *Carcinogenesis*, **16**, 2045–2050.
7. Yermilov, V., Rubio, J. & Ohshima, H. (1995). Formation of 8-nitroguanine in DNA treated with peroxynitrite *in vitro* and its rapid removal from DNA by depurination. *FEBS Lett.* **376**, 207–210.
8. Lewis, R. S., Tannenbaum, S. R. & Deen, W. M. (1995). Kinetics of N-nitrosation in oxygenated nitric oxide solutions at physiological pH: role of nitrous anhydride and effects of phosphate and chloride. *J. Am. Chem. Soc.* **117**, 3933–3939.
9. Wink, D. A., Kasprzak, K. S., Maragos, C. M., Elespuru, R. K., Misra, M., Dunams, T. M. *et al.* (1991). DNA deaminating ability and genotoxicity of nitric oxide and its progenitors. *Science*, **254**, 1001–1003.
10. Nguyen, T., Brunson, D., Crespi, C. L., Penman, B. W., Wishnok, J. S. & Tannenbaum, S. R. (1992). DNA damage and mutation in human cells exposed to nitric oxide *in vitro*. *Proc. Natl Acad. Sci. USA*, **89**, 3030–3034.
11. Caulfield, J. L., Wishnok, J. S. & Tannenbaum, S. R. (1998). Nitric oxide-induced deamination of cytosine and guanine in deoxynucleosides and oligonucleotides. *J. Biol. Chem.* **273**, 12689–12695.
12. Dong, M., Wang, C., Deen, W. M. & Dedon, P. C. (2003). Absence of 2'-deoxyoxanosine and presence of abasic sites in DNA exposed to nitric oxide at controlled physiological concentrations. *Chem. Res. Toxicol.* **16**, 1044–1055.
13. Pang, B., Zhou, X., Yu, H., Dong, M., Taghizadeh, K., Wishnok, J. S. *et al.* (2007). Lipid peroxidation dominates the chemistry of DNA adduct formation in a mouse model of inflammation. *Carcinogenesis*, **28**, 1807–1813.
14. Dong, M. & Dedon, P. C. (2006). Relatively small increases in the steady-state levels of nucleobase deamination products in DNA from human TK6 cells exposed to toxic levels of nitric oxide. *Chem. Res. Toxicol.* **19**, 50–57.
15. Gal, A. & Wogan, G. N. (1996). Mutagenesis associated with nitric oxide production in transgenic SJL mice. *Proc. Natl Acad. Sci. USA*, **93**, 15102–15107.
16. Kamiya, H., Sakaguchi, T., Murata, N., Fujimuro, M., Miura, H., Ishikawa, H. *et al.* (1992). *In vitro* replication study of modified bases in ras sequences. *Chem. Pharm. Bull.* **40**, 2792–2795.
17. Masutani, C., Araki, M., Yamada, A., Kusumoto, R., Nogimori, T., Maekawa, T. *et al.* (1999). Xeroderma pigmentosum variant (XP-V) correcting protein from HeLa cells has a thymine dimer bypass DNA polymerase activity. *EMBO J.* **18**, 3491–3501.
18. Ogi, T., Kato, T., Jr, Kato, T. & Ohmori, H. (1999). Mutation enhancement by DINB1, a mammalian homologue of the *Escherichia coli* mutagenesis protein dinB. *Genes Cells*, **4**, 607–618.
19. Gerlach, V. L., Aravind, L., Gotway, G., Schultz, R. A., Koonin, E. V. & Friedberg, E. C. (1999). Human and mouse homologs of *Escherichia coli* DinB (DNA polymerase IV), members of the UmuC/DinB superfamily. *Proc. Natl Acad. Sci. USA*, **96**, 11922–11927.
20. Goodman, M. F. & Tippen, B. (2000). The expanding polymerase universe. *Nat. Rev., Mol. Cell Biol.* **1**, 101–109.
21. Kunkel, T. A., Pavlov, Y. I. & Bebenek, K. (2003). Functions of human DNA polymerases η, κ and ι suggested by their properties, including fidelity with undamaged DNA templates. *DNA Repair*, **3**, 135–149.
22. Shibutani, S. (1993). Quantitation of base substitutions and deletions induced by chemical mutagens during DNA synthesis *in vitro*. *Chem. Res. Toxicol.* **6**, 625–629.
23. Shibutani, S., Suzuki, N., Matsumoto, Y. & Grollman, A. P. (1996). Miscoding properties of 3,N^4-etheno-2'-deoxycytidine in reactions catalyzed by mammalian DNA polymerases. *Biochemistry*, **35**, 14992–14998.
24. Mendelman, L. V., Boosalis, M. S., Petruska, J. & Goodman, M. F. (1989). Nearest neighbor influences on DNA polymerase insertion fidelity. *J. Biol. Chem.* **264**, 14415–14423.
25. Mendelman, L. V., Petruska, J. & Goodman, M. F. (1990). Base mispair extension kinetics. Comparison of DNA polymerase alpha and reverse transcriptase. *J. Biol. Chem.* **265**, 2338–2346.
26. Clark, J. M., Joyce, C. M. & Beardsley, G. P. (1987). Novel blunt-end addition reactions catalyzed by DNA polymerase I of *Escherichia coli*. *J. Mol. Biol.* **198**, 123–127.

27. Terashima, I., Suzuki, N., Dasaradhi, L., Tan, C.-K., Downey, K. M. & Shibutani, S. (1998). Translesional synthesis on DNA templates containing an estrogen quinone derived adduct: N^2-(2-hydroxyestron-6-yl)-2'-deoxyguanosine and N^6-(2-hydroxyestron-6-yl)-2'-deoxyadenosine. *Biochemistry*, **37**, 13807–13815.
28. Routledge, M. N., Wink, D. A., Keefer, L. K. & Dipple, A. (1993). Mutations induced by saturated aqueous nitric oxide in the pSP189 *supF* gene in human Ad293 and *E. coli* MBM7070 cells. *Carcinogenesis*, **14**, 1251–1254.
29. Kelman, D. J., Christodoulou, D., Wink, D. A., Keefer, L. K., Srinivasan, A. & Dipple, A. (1997). Relative mutagenicities of gaseous nitrogen oxides in the *supF* gene of pSP189. *Carcinogenesis*, **18**, 1045–1048.
30. Routledge, M. N., Wink, D. A., Keefer, L. K. & Dipple, A. (1994). DNA sequence changes induced by two nitric oxide donor drugs in the *supF* assay. *Chem. Res. Toxicol.* **7**, 628–632.
31. Juedes, M. J. & Wogan, G. N. (1996). Peroxynitrite-induced mutation spectra of pSP189 following replication in bacteria and in human cells. *Mutat. Res.* **349**, 51–61.
32. Kim, M. Y., Dong, M., Dedon, P. C. & Wogan, G. N. (2005). Effects of peroxynitrite dose and dose rate on DNA damage and mutation in the *supF* shuttle vector. *Chem. Res. Toxicol.* **18**, 76–86.
33. Routledge, M. N. (2000). Mutations induced by reactive nitrogen oxide species in the *supF* forward mutation assay. *Mutat. Res.* **450**, 95–105.
34. Suzuki, N., Yasui, M., Geacintov, N. E., Shafirovich, V. & Shibutani, S. (2005). Miscoding events during DNA synthesis past the nitration-damaged base 8-nitroguanine. *Biochemistry*, **44**, 9238–9245.
35. Shibutani, S., Takeshita, M. & Grollman, A. P. (1991). Insertion of specific bases during DNA synthesis past the oxidation-damaged base 8-oxodG. *Nature*, **349**, 431–434.
36. Yasui, M., Suzuki, N., Miller, H., Matsuda, T., Matsui, S. & Shibutani, S. (2004). Translesion synthesis past 2'-deoxyxanthosine, a nitric oxide-derived DNA adduct, by mammalian DNA polymerases. *J. Mol Biol.* **344**, 665–674.
37. Kamiya, H., Miura, H., Kato, H., Nishimura, S. & Ohtsuka, E. (1992). Induction of mutation of a synthetic c-Ha-*ras* gene containing hypoxanthine. *Cancer Res.* **52**, 1836–1839.
38. Yao, M. & Kow, Y. W. (1996). Cleavage of insertion/deletion mismatches, flap and pseudo-Y DNA structures by deoxyinosine 3'-endonuclease from *Escherichia coli*. *J. Biol. Chem.* **271**, 30672–30676.
39. Yao, M., Hatahet, Z., Melamede, R. J. & Kow, Y. W. (1994). Purification and characterization of a novel deoxyinosine-specific enzyme, deoxyinosine 3' endonuclease, from *Escherichia coli*. *J. Biol. Chem.* **269**, 16260–16268.
40. Yao, M. & Kow, Y. W. (1995). Interaction of deoxyinosine 3'-endonuclease from *Escherichia coli* with DNA containing deoxyinosine. *J. Biol. Chem.* **270**, 28609–28616.
41. Saparbaev, M. & Laval, J. (1994). Excision of hypoxanthine from DNA containing dIMP residues by the *Escherichia coli*, yeast, rat, and human alkylpurine DNA glycosylases. *Proc. Natl Acad. Sci. USA*, **91**, 5873–5877.
42. Fortini, P., Parlanti, E., Sidorkina, O. M., Laval, J. & Dogliotti, E. (1999). The type of DNA glycosylase determines the base excision repair pathway in mammalian cells. *J. Biol. Chem.* **274**, 15230–15236.
43. Miao, F., Bouziane, M. & O'Connor, T. R. (1998). Interaction of the recombinant human methylpurine-DNA glycosylase (MPG protein) with oligodeoxyribonucleotides containing either hypoxanthine or abasic sites. *Nucleic Acids Res.* **26**, 4034–4041.
44. Schouten, K. A. & Weiss, B. (1999). Endonuclease V protects *Escherichia coli* against specific mutations caused by nitrous acid. *Mutat. Res.* **435**, 245–254.
45. Weiss, B. (2006). Evidence for mutagenesis by nitric oxide during nitrate metabolism in *Escherichia coli*. *J. Bacteriol.* **188**, 829–833.
46. Guo, G. & Weiss, B. (1998). Endonuclease V (*nfi*) mutant of *Escherichia coli* K-12. *J. Bacteriol.* **180**, 46–51.
47. Dong, M., Vongchampa, V., Gingipalli, L., Cloutier, J. F., Kow, Y. W., O'Connor, T. & Dedon, P. C. (2006). Development of enzymatic probes of oxidative and nitrosative DNA damage caused by reactive nitrogen species. *Mutat. Res.* **594**, 120–134.
48. Weiss, B. (2001). Endonuclease V of *Escherichia coli* prevents mutations from nitrosative deamination during nitrate/nitrite respiration. *Mutat. Res.* **461**, 301–309.
49. Kawase, Y., Iwai, S., Inoue, H., Miura, K. & Ohtsuka, E. (1986). Studies on nucleic acid interactions. I. Stabilities of mini-duplexes (dG2A4XA4G2–dC2T4YT4C2) and self-complementary d(GGGAAXYTTCCC) containing deoxyinosine and other mismatched bases. *Nucleic Acids Res.* **14**, 7727–7736.
50. Uesugi, S., Oda, Y., Ikehara, M., Kawase, Y. & Ohtsuka, E. (1987). Identification of I:A mismatch base-pairing structure in DNA. *J. Biol. Chem.* **262**, 6965–6968.

Radiat Environ Biophys (2008) 47:439–444
DOI 10.1007/s00411-008-0179-7

ORIGINAL PAPER

Repair of I-SceI Induced DSB at a specific site of chromosome in human cells: influence of low-dose, low-dose-rate gamma-rays

Fumio Yatagai · Masao Suzuki · Noriaki Ishioka · Hitoshi Ohmori · Masamitsu Honma

Received: 9 January 2008 / Accepted: 5 June 2008 / Published online: 21 June 2008
© Springer-Verlag 2008

Abstract We investigated the influence of low-dose, low-dose-rate gamma-ray irradiation on DNA double strand break (DSB) repair in human lymphoblastoid TK6 cells. A single DSB was introduced at intron 4 of the *TK+* allele (chromosome 17) by transfection with the I-SceI expression vector pCBASce. We assessed for DSB repair due to non-homologous end-joining (NHEJ) by determining the generation of TK-deficient mutants in the TK6 derivative TSCE5 (*TK +/−*) carrying an I-SceI recognition site. We similarly estimated DSB repair via homologous recombination (HR) at the same site in the derived compound heterozygote (*TK−/−*) cell line TSCER2 that carries an additional point mutation in exon 5. The NHEJ repair of DSB was barely influenced by pre-irradiation of the cells with 30 mGy γ-rays at 1.2 mGy h^{-1}. DSB repair by HR, in contrast, was enhanced by ~50% after pre-irradiation of the cells under these conditions. Furthermore, when I-SceI digestion was followed by irradiation at a dose of 8.5 mGy, delivered at a dose rate of only 0.125 mGy h^{-1}, HR repair efficiency was enhanced by ~80%. This experimental approach can be applied to characterize DSB repair in the low-dose region of ionizing radiation.

F. Yatagai (✉) · H. Ohmori
Advanced Development and Support Center,
The Institute of Physical and Chemical Research (RIKEN),
Saitama 351-0198, Japan
e-mail: yatagai@postman.riken.go.jp

M. Suzuki
Heavy-ion Medical Science Center,
National Institute of Radiological Sciences,
Chiba-shi, Chiba, Japan

N. Ishioka
Japan Aerospace Exploration Agency,
Institute of Space and Astronautical Science,
Tsukuba-shi, Ibaraki, Japan

M. Honma
Division of Genetics and Mutagenesis,
National Institute of Health Sciences, Tokyo, Japan

Introduction

Health risks from low doses of ionizing radiation (IR) are of concern and it is important to estimate such risks for persons occupationally exposed to IR, such as airline crews, astronauts, and some workers in medical and industrial fields, including those in nuclear plants. Genetic analyses for induction of mutations, chromosome aberrations, micronuclei etc., are frequently used to estimate radiation risk. A new sensitive methodology developed in Honma's laboratory—analysis of loss of heterozygosity (LOH) at the *thymidine kinase* (*TK*) locus in human lymphoblastoid TK6 cells [1, 2]—can detect LOH events (interstitial deletions) in cells exposed to low doses of γ-rays delivered at a low dose rate, such as 30 mGy delivered at 1.2 mGy h^{-1} [3]. The LOH events are most likely a consequence of inaccurate repair of DNA double-strand breaks (DSBs), the most dangerous DNA lesion induced by IR. The high frequency of interstitial deletions observed after a low dose (30 mGy) exposure was unexpected because the estimated probability of generating two DSBs in the *TK* locus region is low under these conditions ($<2.25 \times 10^{-10}$) [3]. Thus, the radiation-induced DSBs seem unlikely to initiate the interstitial deletions. Rather, the deletions might result from IR interfering with correct repair of spontaneous DSBs or from the conversion of other damage, such as single-strand breaks.

When we tried to explore the influence of low-dose IR on DSB repair, we found it difficult to track specifically DSBs

amid the variety of DNA lesions that were induced. We therefore constructed a model system that could trace the fate of a single DSB [4, 5]. Our system can distinguish two major DSB repair pathways, non-homologous end-joining (NHEJ) and homologous recombination (HR) [6, 7]. NHEJ joins broken ends, which have little or no sequence homology in a non-conservative manner, and some information may be lost in the course of the repair process. HR, on the other hand, requires extensive tracts of sequence homology and is generally considered as error-free [8].

The human cell line TSCE5 is heterozygous (+/−) for the *TK* gene and the line TSCER2 is compound heterozygous (−/−); both carry an I-SceI endonuclease recognition site in intron 4 of one allele of the *TK* gene. DSBs can be generated at the I-SceI site by expression of the I-SceI vector [4]. When DSBs occur at the *TK* locus, NHEJ in TSCE5 cells produces TK-deficient mutants while HR between the *TK* alleles in TSCER2 cells produces TK-proficient revertants. This means that positive–negative drug selection for TK phenotypes permits distinction between NHEJ and HR repair.

The LOH analysis of TK mutants suggests that low-dose, low-dose-rate IR has important indirect effects. When the I-SceI model system is applied to estimating the influence of low-level IR on repair of a specifically introduced DSB, we can estimate the indirect effects of the exposure because the IR-damaged site can be ignored as a repair target. Here, we first examined whether such indirect effect can be detected by an experiment based upon the original concept of radioadaptation, a priming exposure to low-dose, low-dose-rate IR followed by the challenging treatment of I-SceI digestion. Second, a new type of experiment, the I-SceI treatment followed by low-dose, low-dose-rate IR exposure, was performed to investigate certain kinds of indirect effect, such as an influence of high radiation background exposure on DSB repair, because the continuous expression of I-SceI vector after the cell transfection mimics the above situation. These experiments provided the interesting finding that low level IR enhances the HR pathway.

Materials and methods

Cell line construction

Figure 1 outlines the structure of the repair substrates and the cell lines; the details of the strain construction were described previously [4]. Briefly, in lymphoblastoid TK6 cells heterozygous for the TK gene, the functional allele was first inactivated by gene targeting with vector pTK4 to replace exon 5 of the *TK* gene by a *neo* gene. To introduce the I-SceI recognition site, in a second step the targeting vector, pTK10, encompassing about 6 kb of the original *TK* gene with exons 5, 6, and 7, and the I-SceI recognition site in intron 4, 75 bp upstream of exon 5, was used to revert the *TK* gene disrupted by pTK4. The new line was termed TSCE5. A spontaneous reversion in a TSCE5 cell (G to A in position 23 of exon 5), which we cloned, led to the compound heterozygote (*TK*−/−) cell line, TSCER2. In TSCE5, when a DSB at the I-SceI site is repaired by NHEJ involving a deletion in the adjacent exon, the cell can be isolated as a TK-deficient mutant. In TSCER2, when a DSB is repaired by HR between the *TK* alleles, a TK^+ allele can be generated, resulting in a revertant phenotype.

Cell culture and IR exposure

Cell culture details were described in earlier work [1–3]. We tested the response of TSCE5 and TSCER2 cells cultured in RPMI1640 medium to low-dose, low-dose-rate γ-irradiation in a 5% CO_2 incubator both before (mode A, Fig. 2) and after (mode B, Fig. 2) I-SceI digestion. In mode A, the cells were exposed to ^{60}Co γ-rays at 1.2 mGy h^{-1} for 25 h (total exposure, 30 mGy) and reached a cell concentration of 8×10^5 ml^{-1} at the end of the irradiation/culture period. Then, 2 h after finishing the γ-irradiation, the cells were transfected with the I-SceI expression vector. The delay occurred because the radiation exposure facility was located far from the biological experimental area. In mode B, the cells were transfected with the vector first and 2 h later exposed to a much lower γ-ray dose and dose-rate ($\sim$28% of the mode A dose at $\sim$10% of the mode A dose rate), namely 0.125 mGy h^{-1} for 68 h (total exposure, 8.5 mGy). In an independent determination performed with 8 cell culture flasks in duplicate experiments, cells were exposed for 96 h (total exposure, 12 mGy). At the end of irradiation/culture period in mode B, the cell concentration was adjusted to 8×10^5 ml^{-1}. Control cells were treated in the same manner except that they were not irradiated. The γ-irradiations were performed at the National Institute of Radiological Studies (NIRS), and the adjustment of dose-rate was done by changing the distance between the ^{60}Co source and the CO_2 incubator.

I-SceI expression

We introduced the I-SceI expression vector (pCBASce) by suspending 5×10^6 cells in 0.1 ml Nucleofector Solution V (amaxa AG, Cologne, Germany) with 50 μg of uncut pCBSce vector, or without the vector as a control, following the manufacturer's recommendations [5]. Although we could not determine the efficiency of DSB generation under the present condition of transfection, the I-SceI expression vector was introduced into about 65% of the cells at 24 h after the transfection and the expression lasts for 3 days incubation [5].

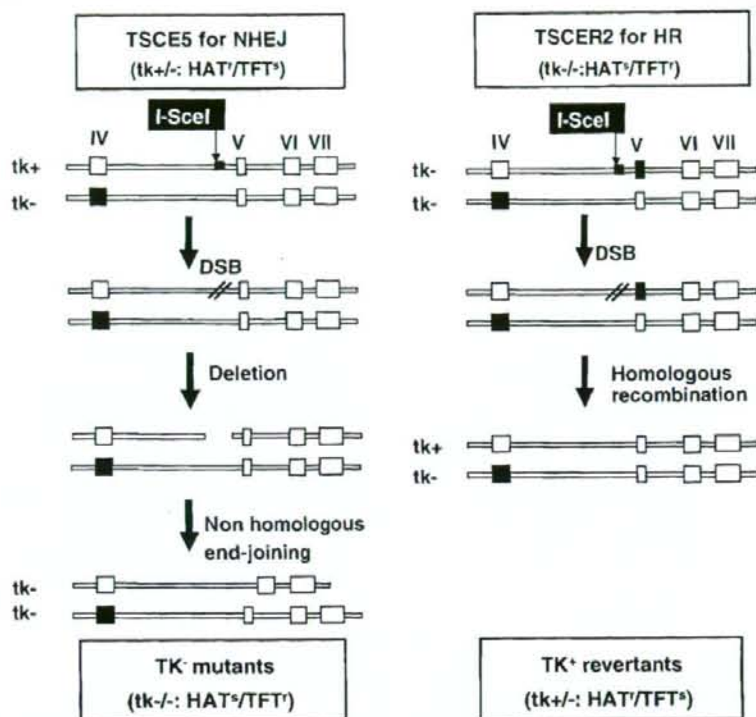

Fig. 1 Strategy of DSB repair assays for I-SceI double strand breaks. The two constructed cell lines—the original TSCE5 line containing the I-SceI recognition insert and its derived compound heterozygote TSCER2—are shown together with the selectable phenotypes generated by repair of double strand breaks (DSBs) through non-homologous end-joining (NHEJ) in TSCE5 cells or homologous repair (HR) in TSCER2 cells (see text)

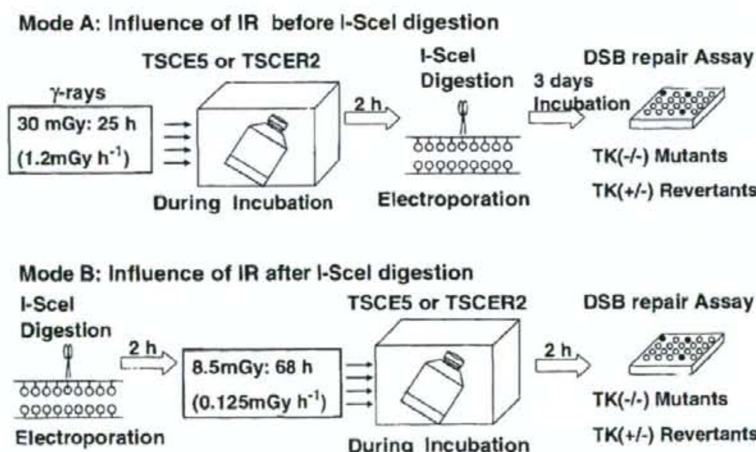

Fig. 2 Experimental scheme of radiation exposure and I-SceI expression. In mode A, cells were exposed to low-dose, low-dose-rate γ-irradiation and then transfected with the I-SecI vector by electroporation (see text). In *mode B* cells were transfected with the I-SceI vector and then exposed to γ-irradiation at a much lower dose and dose-rate (see text)

Determination of TK^- mutants and TK^+ revertants

In mode A, immediately after transfection the cells were suspended in 50 ml of fresh RPMI1640 medium, incubated for 3 days, and then seeded into 96-microwell plates. In mode B, the cell seeding was done at 2 h after the irradiation/incubation following the I-SceI digestion as described above. TSCE5 cells were seeded at 100 cells per well and incubated in the presence of 2.0 $\mu g\ ml^{-1}$ trifluorothymidine (TFT) for the detection of TK-deficient

mutants. TSCER2 cells were seeded at 2,000 cells per well in the presence of HAT (200 μM hypoxanthine, 0.1 μM aminopterin, 17.5 μM thymidine) for the detection of TK-proficient revertants.

Results

TK mutant frequency after γ-irradiation

Table 1a shows frequencies of TK^- mutants in TSCE5 cells not expressing I-SceI without irradiation (control) and after exposure to 30 mGy γ-irradiation at 1.2 mGy h^{-1} (mode A). The mean TK^- mutant frequency (MF) values were found to be 2.7×10^{-6} and 4.7×10^{-6} for control and γ-irradiated sample, respectively, and both the level of MFs and the increase caused by γ-irradiation were consistent with those of a previous investigation [3]. Table 2a shows TK^- mutant frequency in unirradiated control TSCE5 cells and cells that were exposed to 8.5 mGy γ-irradiation at 0.125 mGy h^{-1} (mode B). The mean TK^- MF values for un- and γ-irradiated cells in the mode B experiment (3.0×10^{-6} and 2.1×10^{-6}, respectively) were very similar to values obtained after the 12 mGy exposure (at the same dose-rate as in mode B), namely 3.2×10^{-6} and 2.0×10^{-6} for un- and γ-irradiated sample, respectively. These results suggest that the lower doses (8.5 and 12 mGy) delivered at a lower does rate (0.125 mGy h^{-1}) did not enhance the TK^- mutant frequency but rather reduced it. We did not determine the frequency of TK^+ revertants for unirradiated control and γ-irradiated TSCER2 cells because we expected those frequencies to be too low for us to accurately estimate the effect of IR exposure. In fact, the spontaneous revertant frequency (RF) in TSCER2 is in the range of 10^{-8} [4, 5].

Effect of radiation exposure prior to I-SceI transfection on DSB repair (mode A)

In the mode A experiment, the low-dose, low-dose-rate γ-irradiation was performed prior to transfection with the I-SceI vector to estimate the influence of pre-IR exposure on repair of I-SceI introduced DSB. We calculated the relative TK^- mutant frequency MF_{rel} = (MF (γ-rays + I-SceI)/MF (I-SceI)) for each experiment because the transfection efficiencies varied. The mean MF_{rel} in TSCE5 cells exposed to IR prior to transfection was 1.0 (Table 1a), indicating that irradiation had no effect on NHEJ repair of I-SceI-induced DSBs. The relative TK^+ revertant frequency, RF_{rel} in TSCER2 cells was determined in an analogous manner. Exposure to irradiation prior to transfection consistently enhanced RF_{rel}, and the mean RF_{rel} was 1.5 (Table 1b), indicating that irradiation enhanced the HR repair of DSBs by 50%. This 50% increase was found to be statistically significant by *t*-test ($P = 0.021$, if taken as paired data).

Table 1 Effect on DSB repair of exposure to 30 mGy IR at 1.2 mGy h^{-1} prior to transfection with I-SceI expression vector (mode A)

a) NHEJ efficiency in TSCE5 cells

Exp.	TK^- Mutant Frequency, MF ($\times 10^{-6}$)				Effect of IR (MF_{rel}[a])
	Control	γ-rays	I-SceI	γ-rays + I-SceI	
1	3.5	6.1	8,600	8,500	0.99
2	1.8	3.2	2,900	3,200	1.1
Mean	2.7	4.7	5,800	5,900	1.0 ($P = 0.82$)[c]

b) HR efficiency in TSCER2 cells

Exp.	TK^+ Revertant Frequency, RF ($\times 10^{-6}$)				Effect of IR (RF_{rel}[b])
	Control	γ-rays	I-SceI	γ-rays + I-SceI	
1	–	–	90	114	1.3
2	–	–	62	96	1.5
3	–	–	25	45	1.8
Mean	–	–	59	85	1.5 ($P = 0.021$)[c]

[a] MF_{rel} was calculated as MF (γ-rays + I-SceI)/MF (I-SceI)

[b] RF_{rel} was calculated as RF (γ-rays + I-SceI)/RF (I-SceI)

[c] Assuming that they were paired data, *P* value was calculated by *t*-test

Table 2 Effect on DSB repair of exposure to 8.5 mGy IR at 0.125 mGy h^{-1} following transfection with I-SceI expression vector (mode B)

a) NHEJ efficiency in TSCE5 cells

Exp.	TK^- Mutant Frequency, MF ($\times 10^{-6}$)				Effect of IR (MF_{rel}[a])
	Control	γ-rays	I-SceI	γ-rays + I-SceI	
1	2.8	1.3	3,400	4,500	1.3
2	3.1	2.8	12,000	17,000	1.4
3	–	–	11,000	11,000	1.0
Mean	3.0	2.1	8,800	10,800	1.2 ($P = 0.12$)[c]

b) HR efficiency in TSCER2 cells

Exp.	TK^+ Revertant Frequency, RF ($\times 10^{-6}$)				Effect of IR (RF_{rel}[b])
	Control	γ-rays	I-SceI	γ-rays + I-SceI	
1	–	–	82	160	2.0
2	–	–	160	270	1.7
3	–	–	110	190	1.7
Mean	–	–	120	210	1.8 ($P = 0.0013$)[c]

[a] MF_{rel} was calculated as MF (γ-rays + I-SceI)/MF (I-SceI)

[b] RF_{rel} was calculated as RF (γ-rays + I-SceI)/RF (I-SceI)

[c] Assuming that they were paired data, *P* value was calculated by *t*-test

Effect of radiation exposure after I-SceI transfection on DSB repair (Mode B)

In the mode B experiment, the γ-irradiation was performed after transfection with the I-SceI vector to estimate the post-IR exposure effects on DSB repair. The mean MF_{rel} in TSCE5 cells exposed to IR following transfection was 1.2 (Table 2a) and the difference between unirradiated and irradiated cells was not statistically significant, indicating that post-transfection γ-irradiation had hardly any effect on NHEJ repair of DSBs. The mean RF_{rel} in TSCER2 cells under the same conditions, however, was 1.8 (Table 2b), indicating that exposure to γ-irradiation following transfection with I-SceI enhanced the HR repair of DSBs by 80%. This 80% increase was also found to be statistically significant by t-test ($P = 0.0013$, if taken as paired data).

Discussion

The efficiency of transfection using the amaxa nucleofection system was estimated to be about 40-fold higher than that using BioRad electroporation system, and this higher efficiency enabled us to more accurately estimate the repair of a single DSB at the specific I-SceI recognition site. As in our previous studies [4, 5], we observed that the frequencies of TK^+ revertants after the I-SceI vector transfection were lower than those of TK^- mutants. That finding seems to be consistent with the notion that NHEJ is the major repair pathway in mammalian cells [9]. Because our I-SceI system does not cover all NHEJ and HR events, it is however difficult to estimate the extent of DSB repair by HR. For example, our system does not cover sister-chromatid HR, which is probably the major HR pathway in mammalian cells. Small gene conversion events, not expanding to the exon 5 region, also cannot be detected by this system. Furthermore, there might be unkown factors, specific to this I-SceI site, which reduce the occurrences of the gene conversion type of events. Although the I-SceI system might over-estimate the repair efficiency of NHEJ compared with HR, it is a good model for elucidating the DSB repair associated with low-dose IR exposure.

Although transfection efficiencies varied from experiment to experiment, the relative TK^- mutant frequency and TK^+ revertant frequency were sufficient for evaluating the influence of IR on DSB repair. Both modes (A and B) of delivering low-dose, low dose-rate γ-irradiation were found to hardly influence NHEJ at the I-SceI site. Since an adaptive mutagenic response, a reduction of TK^- mutation frequency, was observed in TK6 cells exposed to X-rays (5 cGy of priming dose and 2 Gy of challenge dose) [10], we also measured DSB repair in cells in which the challenging X-ray exposure was replaced by I-SceI digestion. In those measurements, similarly, NHEJ was barely influenced by the priming X-ray radiation (unpublished data), suggesting that an acute low-dose IR exposure also might provide the same tendency of "no influence" as that observed with the low-dose, low-dose-rate γ-irradiation. In contrast to NHEJ, both modes of γ-irradiation in the present experiments were found to considerably enhance HR at the I-SceI sites. This enhanced HR was not due to radiation-induced S/G2 arrest, because the low-dose IR did not affect the cell cycle (data not shown). Similar results were obtained when using a priming X-radiation (5 cGy; unpublished data).

The above similarities suggest that the enhancement of HR repair observed in the present study is a manifestation of an adaptive response where the low-dose, low-dose-rate γ-irradiation was the priming exposure. The inefficient effect of γ-irradiation on NHEJ does not seem to be consistent with a higher efficiency of DSB repair in radioadapted cells [11], as was shown by the reduction of genetic alterations at the chromosome level [12–14]. Since IR-induced DSBs were the major targets for adaptation in those studies, their DSBs might differ in some way from the I-SceI-induced DSBs we report on here. In other words, the fate of site-specific I-SceI breaks might reflect repair of spontaneous DSBs more faithfully than that of DSBs induced directly by relatively high dose exposure. At the present stage, it is very difficult to speculate plausible mechanisms responsible for the apparent adaptive response of DSB repair. We believe that the characteristics of I-SceI breaks and their continuous generation after the transfection are related to the observed repair characteristics. The enhanced repair by HR upon low-dose, low-dose-rate γ-irradiation is obviously not due to an enhanced cleavage of the I-SceI site after irradiation, since we have not observed such enhanced repair by NHEJ.

It remains to be tested whether NHEJ is really not enhanced by low-dose, low-dose-rate IR or whether it apparently remained stable because of limitations of the methodology. Recently, the fates of I-SceI breaks located in TSCE5 cells were determined in randomly isolated clones using non-phenotypic selection [5]. About 97% of the clones showed perfect rejoining, and deletions corresponding to the events detectable by the present selection method (i.e. large enough to affect the adjacent exon) were found in only 0.54% of the clones. Thus, if perfect NHEJ events or small deletion events were enhanced by low-dose, low-dose-rate γ-irradiation, we would not detect them by the present methodology.

In addition, the mechanisms responsible for HR repair, which is active in S/G2 phase cells, remains to be elucidated. In our previous studies using genetic analyses, we observed small homozygous LOH events in primed cells in the X-ray plus X-ray radioadaptive experiment mentioned

above [10]. We observed the same pattern of LOH mutants after low-dose, low-dose-rate γ-ray exposures [3], although the frequency was low. These results can be explained by the enhanced contribution of HR observed in the I-SceI digestion system, because this system could recover the non-crossing over gene conversion events very efficiently among the TK^+ revertants. In near future we need to elucidate HR pathway leading to gene conversion, where a central core of protein, most likely the RecA homolog RAD51, plays a key role [15].

DSBs arise from endogenous sources including reactive oxygen species generated during cellular metabolisms. The DSB generation process mediated by reactive oxygen is suggested to be also involved in the indirect effects of the ionizing radiation exposure. As already described, the site-specific I-SceI break in our system can be considered as a good model for endogeneous DSBs. Thus, enhanced HR repair activity induced by low-dose, low-dose-rate IR, might be regarded as defense machinery against DNA damage, whether occurring spontaneously and/or after low-dose, low-dose rate IR. At present, we are making an effort to apply the I-SceI digestion system for estimating DSB repair in bystander cells.

Acknowledgments This study was partially supported by the Budget for Nuclear Research of the Ministry of Education, Culture, Sports, Science and Technology, and was reviewed by the Atomic Energy Commission of Japan. We thank Dr. Miriam Bloom (SciWrite Biomedical Writing & Editing Services) for professional editing.

References

1. Morimoto S, Kato T, Honma M, Hayashi M, Hanaoka F, Yatagai F (2002) Detection of genetic alterations induced by low-dose X rays: analysis of loss of heterozygosity for *TK* mutation in human lymphoblastoid cells. Radiat Res 157:533–538
2. Morimoto S, Honma M, Yatagai F (2002) Sensitive detection of LOH events in a human cell line after C-ion beam exposure. J Radiat Res 43(Suppl):S163–S167
3. Umebayashi Y, Honma M, Suzuki M, Suzuki H, Shimazu T, Ishioka N, Iwaki M, Yatagai F (2006) Mutation induction in cultured human cells after low-dose and low-dose-rate γ-ray irradiation: detection by LOH analysis. J Radiat Res 48:7–11
4. Honma M, Izumi M, Sakuraba M, Tadokoro S, Sakamoto H, Wang W, Yatagai F, Hayashi M (2003) Deletion, rearrangement, and gene conversion; genetic consequences of chromosomal double-strand breaks in human cells. Environ Mol Mutagen 42:288–298
5. Honma M, Sakuraba M, Koizumi T, Takashima T, Sakamoto H, Hayashi M (2007) Non-homologous end-joining for repairing I-SceI induced DNA double strand breaks in human cells. DNA Repair 6:781–788
6. Jackson SP (2002) Sensing and repairing DNA double-strand breaks. Carcinogenesis 23:687–696
7. Valerie K, Povirk LF (2003) Regulation and mechanisms of mammalian double-strand break repair. Oncogene 22:5792–5812
8. Jeggo PA (1998) DNA breakage and repair. Adv Genet 38:185–282
9. Pastwa E, Blasiak J (2003) Non-homologous end-joining. Acta Biochim Pol 50:891–908
10. Yatagai F, Umebayashi Y, Honma M, Sugasawa K, Takayama Y, Hanaoka F (2007) Mutagenic radioadaptation in a human lymphoblastoid cell line. Mutat Res 638:48–55
11. Ikushima T, Aritomi H, Morisita J (1996) Radioadaptive response: efficient repair of radiation-induced DNA damage in adapted cells. Mutat Res 358:193–198
12. Rigaud O, Papadopoulo D, Moustacchi E (1993) Decreased deletion mutation in radioadapted human lymphoblast. Radiat Res 133:94–101
13. Azzam EI, Raaphorst GP, Mitchel RE (1994) Radiation-induced adaptive response for protection against micronucleus formation and neoplastic transformation in C3H 10T1/2 mouse embryo cells. Radiat Res 138:S28–S31
14. Ueno AM, Vannais DB, Gustafson SL, Wong JC, Waldren CA (1996) A low adaptive dose of gamma-rays reduced the number and altered the spectrum of S1 mutants in human hamster hybrid cells. Mutat Res 358:161–169
15. Li X, Heyer W-D (2008) Homologous recopmbination in DNA repair and DNA damage tolerance. Cell Res 18:99–113

Genes and Environment, Vol. 30, No. 4 pp. 101-107 (2008)

Meeting report

International Symposium on Genotoxic and Carcinogenic Thresholds

Takehiko Nohmi[1,3], Naomi Toyoda-Hokaiwado[1], Masami Yamada[1], Kenichi Masumura[1], Masamitsu Honma[1] and Shoji Fukushima[2]

[1]Division of Genetics and Mutagenesis, National Institute of Health Sciences, Tokyo, Japan
[2]Japan Bioassay Research Center, Japan Industrial Safety and Health Association, Kanagawa, Japan

(Received October 17, 2008; Accepted November 10, 2008)

Rodent toxicity assays are usually conducted at high doses based on the maximum tolerable doses. Since the doses used for the assays are sometime 1,000 or 10,000 times higher than the levels at which humans are actually exposed, it is questioned whether carcinogenicity observed at high doses can be observed at low doses. In regulatory sciences, a default assumption for chemical carcinogens is that carcinogenicity observed at high doses can be linearly extrapolated to low doses without thresholds when genotoxicity (or DNA reactivity) is involved in the mechanisms of carcinogenesis. This means that genotoxic carcinogens impose cancer risk to humans even at very low doses. Genotoxicity is a property of chemicals that can interact with DNA, thereby inducing mutations and chromosome aberrations. These genetic alterations are generally thought as molecular basis of carcinogenesis. Recently, the assumption, i.e., the linear non-threshold (LNT) model for chemical carcinogens, has been challenged by several lines of experimental evidence where a large scale of rodents is employed to generate dose-response curves that suggest the presence of practical thresholds. In addition, the LNT assumption appears counterintuitive because it is well known that humans possess a variety of defense mechanisms against genotoxic and carcinogenic insults. The defense mechanisms include detoxication metabolism, error-free DNA repair and translesion DNA synthesis, apoptosis and so on. These mechanisms may effectively suppress genotoxic and carcinogenic activities of chemicals, thereby constituting "practical" thresholds for genotoxic and carcinogenic chemicals. To discuss the low dose effects of genotoxic and carcinogenic compounds and the implication in regulatory sciences, International Symposium on Genotoxic and Carcinogenic Thresholds has been held in Tokyo on July 22 and 23, 2008. Since the topic is related to multi expert areas, 21 scientists including five oversea speakers were invited from various scientific fields such as genotoxicology, chemical pathology, radiation biology, analytical chemistry, statistics and drug metabolism. An administrative official and a representative of consumers were also invited. Here, we summarize the presentations of the symposium to discuss future perspectives in the threshold issue of genotoxic and carcinogenic compounds.

Session 1 (chaired by Makoto Hayashi and Shoji Fukushima)

Opening Address

Takehiko Nohmi (National Institute of Health Sciences, Japan)

Nohmi declared the opening of the symposium and introduced basic concepts related to thresholds for genotoxic and carcinogenic compounds. Currently, carcinogens are classified into "genotoxic" and "non-genotoxic". The genotoxic carcinogens are DNA reactive and induce cancer in multiple organs in trans-species of rodents. They are usually positive in some of *in vitro* and *in vivo* tests of genotoxicity. In contrast, non-genotoxic carcinogens induce tumors in a variety of mechanisms other than DNA damage. The mechanisms include hormonal effects, cytotoxicity and inflammation and so on. The classification, i.e., genotoxic or non-genotoxic, has relevance in administrative regulation of chemicals because it is assumed that genotoxic carcinogens have no thresholds in cancer risk and therefore no ADI (acceptable daily intake) can be set for genotoxic carcinogens. Nohmi questioned the scientific basis for the regulatory policy since it is well known that humans possess multiple defense mechanisms to detoxify genotoxic carcinogens. He stressed the importance of mechanistic understanding of genotoxic carcinogens at low doses to solve the issue of genotoxic and carcinogenic thresholds.

[3]Correspondence to: Takehiko Nohmi, Division of Genetics and Mutagenesis, National Institute of Health Sciences, 1-18-1 Kamiyoga, Setagaya-ku, Tokyo 158-8501, Japan. Tel: +81-3-3700-9872, Fax: +81-3-3700-2348, E-mail: nohmi@nihs.go.jp

© The Japanese Environmental Mutagen Society

1. Possible Mechanisms of Genotoxic Thresholds

Takehiko Nohmi (National Institute of Health Sciences, Japan)

Genomic DNA is continuously exposed to endogenous and exogenous genotoxic compounds and thus mutations and chromosome aberrations are inevitably induced at some extent even without external treatments to damage DNA. Nohmi pointed out that spontaneous mutations play important roles in carcinogenesis and also that endogenous DNA damage is a critical factor for estimation of biological and statistical significance of small increases in mutations at low doses. Nohmi showed experimental evidence that error-free DNA repair constitutes "practical thresholds" for genotoxicity of chemicals using mutants of Ames tester strains that are deficient in repair capacity to DNA damage. The mutants include derivatives of *Salmonella typhimurium* deficient in O^6-methylguanine DNA methyl transferase ($\Delta ada\Delta ogt$), 8-oxo-guanine DNA glycosylase ($\Delta mutM$) or endonuclease III and VIII ($\Delta nth\Delta nei$). These strains exhibit hypersensitivity to mutagenicity of alkylating agents ($\Delta ada\Delta ogt$), oxidizing agents that damage purine bases ($\Delta mutM$) or pyrimidines bases ($\Delta nth\Delta nei$) in DNA. He mentioned that error-free translesion DNA synthesis catalyzed by specialized DNA polymerases may play important roles in constitution of the practical thresholds. It is now known that humans possess more than 14 DNA polymerases per cell and about half are involved in DNA repair and translesion DNA synthesis. Finally, he introduced *gpt* delta transgenic mouse/rat models for *in vivo* genotoxicity. In particular, *gpt* delta transgenic rat may be important to identify genotoxicity (or mutations) in target organs in carcinogenicity.

2. Evidence of Thresholds in Genotoxic Carcinogens: Evidence Based on Carcinogenic Mechanism

Shoji Fukushima (Japan Bioassay Research Center)

Fukushima reported low dose carcinogenicity and genotoxicity of heterocyclic amines, i.e., 2-amino-3,8-dimethylimidazo[4,5-*f*]quinoxaline (MeIQx), 2-amino-3-methylimidazo[4,5-*f*]quinoline (IQ) and amino-1-methyl-6-phenylimidazo[4,5-*b*]pyridine (PhIP), and *N*-nitroso compounds, i.e., dimethylnitrosamine (DMN) and diethylnitrosamine (DEN) in rats. When Fischer 344 rats were fed diets containing MeIQx at doses of 0.001 to 100 ppm in a large scale, i.e., 1,200 rats, lowest effective doses were found to be different depending on the biomarkers, i.e., DNA adducts, 0.01 ppm; 8-hydroxyguanine in DNA, 1 ppm; *lacI* mutations, 10 ppm; glutathione *S*-transferase placental form (GST-P) positive foci formation, 100 ppm; cancer in liver, >100 ppm. The results indicate the existence of practical thresholds for the carcinogenicity. Similarly, there were doses below which no tumor formation was observable for IQ, PhIP, DMN and DEM. Since these carcinogens are all genotoxic, it can be concluded that practical thresholds exist at least for some of genotoxic carcinogens. Fukushima also reported that potassium bromate and 1,4-dioxane, which induced kidney and liver tumors in rats via indirect oxidative damage and cytotoxicity, respectively, exhibited perfect thresholds for the carcinogenicity. It is desirable to regulate genotoxic and carcinogenic compounds based on the view point that there are practical thresholds for genotoxic carcinogens.

3. Strategy of the Scientific Committee on Occupational Exposure Limits (SCOEL) of the European Union in the Derivation of Occupational Exposure Limits (OEL) for Carcinogens

Herman M. Bolt (Institut fur Arbeitsphysiologie an der Universitat Dortmund, Germany)

Bolt introduced recommendations by SCOEL for regulation of carcinogenic compounds. According to them, carcinogens can be categorized into four classes. (A) Non-threshold genotoxic carcinogens such as vinyl chloride and dimethyl sulfate. For these compounds, the LNT model can be applied for the low-dose risk evaluation and the regulations may be based on the principle of "as low as reasonably achievable (ALARA)". (B) Genotoxic carcinogens, for which the existence of thresholds cannot be supported by experimental evidence yet. Acrylamide is one of the compounds in this class, and the LNT model may be used as a default assumption. (C) Genotoxic carcinogens with practical thresholds. The examples are formaldehyde, vinyl acetate and trichloroethylene and their OELs are 0.2 ppm, 5 ppm and 10 ppm, respectively. (D) Non-genotoxic or non DNA-reactive carcinogens, for which true (or perfect) thresholds and no observed adverse effect level (NOAEL) can be set. Tumor promoters, spindle poisons, topoisomerase II inhibitors and hormones are typical examples in this class. He stressed the importance to incorporate mechanistic information into regulation of carcinogenic compounds.

4. Threshold of Genotoxicity

Makoto Hayashi (Biosafety Research Center, Foods, Drugs and Pesticides, Japan)

Hayashi reported that statistical power of mouse peripheral blood micronucleus (MN) assay increased when one million cells per animal were analyzed by flow cytometry in comparison to 2,000 cells by manual analysis. Hayashi and his colleagues examined the sensitivity of mouse MN assays with five clastogens, i.e., mitomy-

cin C, Ara-C, colchicine, acrylamide and potassium bromate. Although there were no significant differences in MN induction among mice when 2,000 cells were analyzed, clear differences became apparent when one million cells were analyzed. It indicates that larger sample sizes give higher power of statistics and also that the sensitivity of MN assay can be improved when cells but not animals are considered as evaluation units. However, lowest doses for MN induction by potassium bromate or acrylamide were not changed even after the sample sizes were increased to one million cells per mouse. He also introduced current topics in International Conference on Harmonization of Technical Requirements for Registration of Pharmaceuticals for Human Use (ICH) where test batteries for genotoxicity were being reorganized.

Session 2 (chaired by Samuel M. Cohen and Akiyoshi Nishikawa)

5. *in vivo* Approaches to Study Mechanism of Action of Genotoxic Carcinogens

Akiyoshi Nishikawa (National Institute of Health Sciences, Japan)

Nishikawa reported *in vivo* approaches to study mechanism of action of genotoxic carcinogens. Currently, genotoxicity and carcinogenicity of chemicals are assessed separately by genotoxicity assays, i.e., Ames test, *in vitro* chromosome aberration test (or mouse lymphoma gene mutation test) and mouse MN test, and by long-term rodent carcinogenicity test, respectively. It is uncertain, therefore, to what extent the detected genotoxic potential can contribute to the carcinogenicity. To solve the issue, he utilized *gpt* delta transgenic rats and mice carrying lambda phage EG10 as a reporter for mutations and showed these animals were powerful tools for the evaluation of both genotoxicity and carcinogenicity in the same organs. Interestingly, MX, which is a genotoxic chlorinated water by-product in Ames test, failed to exert genotoxicity or carcinogenicity *in vivo*. On the other hand, dicyclanil, a known non-genotoxic carcinogen, was genotoxic in the liver of female *gpt* delta mouse. He reported these animal models might have great potential to apply for risk assessment of genotoxic carcinogens. Understanding of the detailed mechanism of carcinogenic action would be crucial for more precise risk assessment of genotoxic carcinogens at low doses.

6. Possible Involvement of Adaptation Mechanisms in the Achievement of an Ineffective Dose Range for the Carcinogenicity of Genotoxic Carcinogens

Dai Nakae (Tokyo Metropolitan Institute of Public Health, Japan, Tokyo University of Agriculture, Japan)

Nakae reported that genotoxic carcinogens had ineffective doses for the carcinogenicity and some adaptation mechanisms might contribute to this phenomenon. To demonstrate this postulate, he and his colleagues performed large scale studies using male Fischer 344 Big Blue rats given a 16-week chronic feeding administration of 0.0001 to 1 ppm of genotoxic carcinogen, i.e., DEN. The number and area of GST-P positive foci in liver were significantly increased only at the highest dose of 1 ppm while mutant frequencies were elevated at a dose of 0.001 ppm and the above. Levels of 8-hydroxyguanine were not changed at all doses used. He suggested these findings might indicate the existence of a practical threshold or an ineffective dose range for the carcinogenicity of genotoxic carcinogens. To utilize the DNA adduct as a marker to determine a practical threshold, he concluded it needs validation of large bodies of data.

7. Possible Dose Threshold for Liver Carcinogenesis by Mutagenic Liver Carcinogens

Hiroyuki Tsuda (Nagoya City University Graduate School of Medical Sciences, Japan)

Generally, under industrial exploitation procedure, the development of new chemicals is immediately stopped when their genotoxicity is clarified. However, Tsuda and his colleagues claimed that some genotoxic substances had non-effective doses in long-term animal experiments. He proposed the existence of the biological threshold level for genotoxic liver carcinogens. Tsuda had examined seven chemicals, i.e., 1,4-dioxan, 2,4-diaminotoluene, *N*-nitrosomorpholine, 1,2-dimethylhydrazine, quinoline, 2-nitropropane and carbon tetrachloride, which were produced during manufacturing process of petroleum-related products, with two individual medium-term carcinogenesis assays (Ito-model for promotion assay and Tsuda-model for initiation assay). In these models, GST-P positive foci were used as a marker to detect preneoplastic lesions. Tsuda suggested that biological threshold levels might exist around NOAEL, but interactions between the threshold and biological defense responses were not clear, and concluded that more extensive research is required to clarify the definitive biological threshold level.

8. Thresholds in Genotoxicity and Carcinogenicity: Urinary Bladder Carcinogens

Samuel M. Cohen (University of Nebraska Medical Center, U.S.A.)

Thresholds for carcinogenic risk are a profound theme that requires extensive discussion on the mechanisms from DNA-damage to carcinogenesis. Cohen showed three bladder carcinogens in rodent models and discussed relationships among genotoxicity, cytotoxicity and carcinogenicity. A non-genotoxic substance uracil formed urinary solids which induced cytotoxicity and cancer in a threshold manner. Genotoxic substance 2-acetylaminofluorene (AAF) is DNA reactive and forms bladder DNA adducts in a dose-responsive linear manner. However, the tumor response is non-linear because cytotoxicity at high doses increases cell proliferation, a necessary component for the carcinogenesis. Arsenic is genotoxic and induces bladder cancer in animal models and humans. However, the genotoxicity occurs by indirect mechanisms, not by direct DNA reactivity. Therefore, the genotoxicity may have a threshold, occurring only at high doses. In discussion, he proposed that "DNA reactivity" was a more definitive term than "genotoxicity", because genotoxicity included mechanisms other than DNA reactivity, such as spindle poison or topoisomerase II inhibition. He claimed that it needs careful considerations to use the term of "threshold". He concluded that true threshold should be defined as the levels where zero cancer risks are expected although practical threshold may be valuable for practical purposes.

Session 3 (chaired by Kirk Kitchin and Masao Hirose)

9. Roles of the Food Safety Commission

Masao Hirose (Food Safety Commission, Japan)

Hirose introduced the Food Safety Commission (FSC) in Japan, which was established in 2003, and its major roles, i.e., risk assessment of the hazards contained in foods, risk communication and responses to emergency situations. FSC includes three risk assessment groups for chemical substances, biological materials and emerging foods. FSC has received requests related to risk assessment for more than 1000 items from the risk management organizations such as Ministry of Health, Labour and Welfare, since establishment. The assessments have been completed for about 550 items including 154 pesticides and 165 veterinary medicines. FSC conducts assessment on its own initiative (self-tasks) when the Commission considers issues needed to be evaluated from the analyses of food safety information, public opinion and similar information. FSC follows the classical concept that genotoxic carcinogens do not have threshold levels and thus ADI cannot be applied to genotoxic and carcinogenic compounds added to foods such as food additives and pesticides. From the FSC's point of view, it would not proper to establish ADI to genotoxic compounds.

10. Thresholds for Genotoxic Carcinogens: View from the National Food Safety

Takashi Kunieda (Ministry of Health, Labour, and Welfare, Japan)

Kunieda reported that regulatory approaches to genotoxic carcinogens in food have not been well established yet and thus global consensus-building in this field is needed. Regulation of carcinogens in food is one of major issues in the national food safety program, because cancer deaths account for 30 percent of all deaths in Japan and most consumers have special concerns about the carcinogenicity of substances in food. Non-genotoxic substances do not directly damage DNA, and carcinogenic thresholds are considered to exist. It is possible to ensure the safety of these substances by establishing applicable standards based on the ADI or tolerable dairy intake (TDI). On the other hand, genotoxic substances directly damage DNA, and no carcinogenic thresholds are considered to exist. As the ADI or TDI cannot be established, it is required to individually respond to ensure the food safety from these substances, according to characteristics of them. Risk management is carried out for unavoidable chemicals based on the following risk assessments approaches to reduce human exposure to ALARA: carcinogenic risk calculated by low-dose extrapolation and margin of exposure using the benchmark dose.

11. Consumers View

Kazuo Onitake (Japanese Consumers' Co-operative Union)

Onitake reported the opinion from the consumers' view as a representative of Japanese Consumers' Co-operative Union (JCCU), whose major objective is to protect the health of consumers. JCCU has been addressing many issues related to food safety, such as food additives and residues of agricultural chemicals, for a long period of time. JCCU is of the opinion that when managing risk associated with the use of chemicals or with the presence of chemicals as contaminants from the environment, risk assessments should be performed before any action is taken and other legitimate factors should be taken into consideration. JCCU agrees with the principle that genotoxic carcinogens do not have biological threshold and ADI cannot be applied to those chemicals intentionally added to foods such as food additives, pesticides and veterinary drugs. JCCU believes that this position is responding to the expectations of

consumers who are concerned about any possible risks from genotoxic carcinogens in food.

12. Theoretical and Experimental Approaches to Possible Thresholds of Response in Carcinogenicity

Kirk T. Kitchin (Environmental Protection Agency, U.S.A.)

Kitchin reported that no convincing examples of carcinogenic thresholds in humans are known, except for one theoretical approach, the two-stage clonal growth model by the Moolgavkar group. In animals, at least four good examples of carcinogenic thresholds have been observed. DNA adducts data for the five well studied chemicals were fairly linear while the foci and tumor data show supralinear, linear and threshold curves, making it difficult to generalize. Currently there is no good scientific and regulatory understanding of chemicals that act simultaneously or sequentially via both linear and nonlinear carcinogenic pathways (genotoxic and nongenotoxic). In order to elucidate the dose-response of chemicals of dual carcinogenic dose-response properties (linear and non linear), Kitchin proposes the studies for two or more such chemicals in a large scale coordinated fashion employing at least 1,000 animals, five different treatment groups, six different study parameters and 8 different scientific disciplines.

Session 4 (chaired by David Lovell and Yoshiya Shimada)

13. Modification of Threshold Dose in Radiation-induced Mouse Lymphoma Development

Yoshiya Shimada (National Institute of Radiaological Sciences, Japan)

Shimada reported the studies of radiation-induced mouse thymic lymphoma focusing on dose response of lymphoma induction and the effects of genetic factors, i.e., DNA repair capacity of mouse, and environmental factors, i.e., alkylating agents. The dose limit for radiation protection is based on the LNT hypothesis, where the carcinogenic risk is proportional to radiation dose, even at low doses. However, the results showed that the dose response relationship for mouse thymic lymphomagenesis after repeated X-irradiation has an apparent threshold at dose of around 400 mGy per fraction. DNA repair capacity for double strand breaks or mismatch of nucleotides is a critical determinant for manifestation of threshold.

14. The Progress of Trace Analytical Technique for Measurement of Chemicals in Foods

Munetomo Nakamura (Japan Food Research Laboratories)

Nakamura reported the recent progress of analytical methods using gas chromatograph/mass spectrometer (GC/MS(/MS)) and liquid chromatograph/mass spectrometer (LC/MS(/MS)). In 2006, the positive list system for agricultural chemicals was introduced in Japan. At the same time, many maximum residue limits have been established. Therefore, a lot of analytical methods for residual chemical substances had to be developed. GC/MS(/MS) or LC/MS(/MS) technique can analyze many substances at one time with good selectivity and sensitivity. Those benefits simplify purification steps too. Those methods are adopted as official methods for analysis of pesticide residues in foods, veterinary medicines and carcinogenic and genotoxic mycotoxins.

15. Statistical Consideration on the Identification of Threshold through Toxicological Experiments

Isao Yoshimura (Tokyo University of Science, Japan)

Yoshimura argued that, in principle, it is impossible to identify the threshold via hypothesis testing in the case of toxicological experiments because the probability of false negative decisions cannot be managed in this context. When a mechanism for producing a threshold is hypothesized from a toxicological (or biological) perspective and is mathematically formulated as a dose-response relationship, statistics may be helpful in evaluating the existence (or non-existence) of the threshold. It is important to select a model from a particular set of mathematical dose-response functions. The determination of a practical threshold using *in vitro* experiments may be an alternative to the identification of a "true" threshold, if an appropriate *in vitro* assay affords a large scale experiment at low doses.

16. Statistical Perspective on the Threshold Problem in Toxicological Experiments

David P. Lovell (University of Surrey, U.K.)

Lovell reported mathematical and statistical approaches which do or do not include thresholds and statistical methods which try to identify no observed effect levels (NOELs). There is an increasing appreciation of the potential to identify 'pragmatic' thresholds using experimental systems with a range of biomarkers. The accurate characterization and estimation of these dose-response relationships require careful experimental design which can improve the accuracy of the estimates of the response while avoiding the introduction of ar-

tefactual effects. Statistical approach such as Design of Experiment (DoE) methodology, which builds on the traditional factorial design, can provide efficient approaches for the description and estimation of dose-response relationships of both individual and combinations of agents.

Session 5 (chaired by Minako Nagao and Hansruedi Glatt)

17. Cells Genetically Engineered for Xenobiotic-metabolizing Enzymes: Detection of Genotoxic Effects at Extremely Low Substrate Concentrations

Hansruedi Glatt (German Institute of Human Nutrition, Germany)

Glatt developed Chinese hamster V79 cell lines expressing various human phase-I and phase-II enzymes. Using the transgenic cell lines, he investigated the genotoxicity of a lot of pro-genotoxicants. Human CYP1B1 expressed in the target cell (V79-hCYP1B1) exhibited the genotoxicity of benzo[a]pyrene (BP) at less than 10 nM, while rat liver S9-mediated assay required 7 μM to induce gene mutations. BP induced sister chromatid exchange (SCE) from 10 pM in the cells. The concentration-response curve $[y=f(x)]$ for SCE–unlike for gene mutations–strongly deviated from linearity. Other promutagens required expression of CYP forms different from CYP1B1 and/or non-CYP enzymes (such as sulfotransferases or acetyltransferases) for their activation at low substrate concentrations. In general, compounds requiring expression of non-CYP enzymes in recombinant cells remained inactive in the standard V79/S9 gene mutation assay.

18. Genotoxic consequences of a single double strand break in human cells

Masamitsu Honma (National Institute of Health Sciences, Japan)

Honma mentioned that "threshold of genotoxicity" can not be established, because genotoxicity is generally recognized by experimental assays. Experimentally, thresholds are inferred from dose-reduction experiments in which dosages are decreased to the level at which adverse effects are no longer observed. This strategy demonstrates not a threshold, but rather a detection limit. Ultimately, the most straightforward evidence for a genotoxic threshold would come from examining the effect of a single DNA damage. If this causes mutation, no threshold will exist. If it does not, there will be a threshold for genotoxicity. He developed a novel system to introduce a unique double-strand break (DSB) into the genomic DNA of human cells by restriction enzyme digestion, and demonstrated that 99 % of DSB are repaired by error-prone repair resulting deletion mutations. This result suggested that there is no threshold for genotoxic compounds which cause DSB.

19. Additive Mutagenic Effects of DNA Damages Formed by Multiple Mutagens at Virtually Non-mutagenic Dose Level of Each

Toshihiro Ohta (Tokyo University of Pharmacy and Life Sciences, Japan)

Ohta reported additive mutagenic effects induced by multiple mutagens in which each mutagen did not show mutagenicity at low levels. Six mutagens (furylframide, MX, 4-nitroquinoline *N*-oxide, sodium azide, 1-nitropyrene and captan) induced base-substitution mutations much more efficiently in *Salmonella typhimurium* TA100 (*hisG46, rfa, uvrB*/pKM101), a strain deficient in nucleotide excision repair, than in TA1975P (*hisG46, rfa*/pKM101), a repair proficient strain. Virtually non-mutagenic dose levels were selected by looking for the doses where the chemical was apparently mutagenic to strain TA100 but not to strain TA1975P. The six mutagens were mixed at the virtually non-mutagenic dose level of each and a possible combined mutagenic effect was investigated with strain TA1975P. A significant and reproducible increase in the number of revertants in TA1975P was observed with combined mutagens. Similar investigations were performed using six heterocyclic amines.

20. Consideration on Extension of the Threshold Concept in Animals to Humans

Minako Nagao (Keio University, Japan)

Nagao reported the history of toxicology to reevaluate the presence or absence of threshold in genotoxicity or carcinogenicity. In standard animal carcinogenesis studies, its detection limit is about 10%. In *in vivo* genotoxicity studies, on the other hand, detection limits are about 2-fold of the background. Even if a significant increase in mutation frequency is not observed, mutation spectrum analyses sometimes demonstrate induction of genetic changes. Thus, impacts of the biological responses occurring under the detection limit of an assay system need to be extensively investigated. She also suggested the presence of thresholds in neoplasm induction by PhIP in the colon but not in the breast or hematopoietic system. The presence or the absence of thresholds for a particular carcinogen might be different depending on the target organs. She concluded that clarification of underlying mechanisms would be necessary to confirm presence of threshold.

21. Scientific Implications and Social Impact of Threshold Concept for Genotoxic Carcinogens

Yuzo Hayashi (Japan Health Food & Nutrition Food Association, Japan)

Hayashi discussed the classification of genotoxic and non-genotoxic carcinogens. This classification, however, can not be applied to all instances due to insufficiencies in necessary information. Therefore, the non-threshold concept was introduced exclusively for genotoxic carcinogens and has been adopted in Japan as a basis for regulatory risk assessment. Dose-response studies recently conducted with various genotoxic agents suggest the existence of a threshold. It should be emphasized, however, that a threshold is not a value which can be determined directly from dose-response data. In this context, scientific efforts in support of the adoption of a threshold should be focused on the development of appropriate mathematical models, and the establishment of toxicological concepts. A realistic step towards a paradigm shift from the non-threshold concept is to seek general consensus on the introduction of an appropriate "virtually safe dose" instead of a threshold.

22. Closing Remarks

Shoji Fukushima (Japan Bioassay Research Center)

Fukushima emphasized that evaluation of threshold in carcinogenicity of genotoxic carcinogens is a very important problem in cancer risk assessment and management. Furthermore, various services as well as consumers and industrial workers mutually desire the fast solution of this problem. In the present Symposium, the speakers did the presentations on the matter of risk assessment, risk management and risk communication for free and active discussion as well as exchanging ideas and opinions. Compared to the Symposium organized in two and half years before by Dr. M. Hayashi (NIHS, formerly) and he, in this time more people were gathered and a deeper and mutual comprehension was achieved. It is very important to evaluate the benefit and risk of chemicals on the basis of our latest scientific results and to continue discussion and argumentation on carcinogenic threshold. Furthermore, together with overall look on the problem of threshold, more and more understanding is continuously desired.